

Metal nanoparticles stabilized by cubic silsesquioxanes for catalytic hydrogenations

Xiuli Li,^a Yukou Du,^a Jingtao Dai,^a Xiaomei Wang,^b and Ping Yang^{a,*}

^aCollege of Chemistry and Chemical Engineering, Suzhou 215123, China

^bCollege of Materials Science and Engineering, Soochow University, Suzhou 215021, China

Received 15 April 2007; accepted 17 May 2007

Octa(diacetic aminophenyl) silsesquioxanes (OAAPS) were synthesized and used as stabilizers for preparing metal (Pt, Pd and Ru) nanoparticles using NaBH₄ as a reducing agent. The synthesized catalysts were characterized by UV-vis, XRD, and TEM. The average diameters of Pt (0), Pd (0) and Ru (0) nanoparticles are 1.6 ± 0.3 , 1.4 ± 0.2 and 1.3 ± 0.2 nm, respectively. The metal colloids show excellent stability since OAAPS offer stronger bonding of the cubic linker to the metal nanoparticles through the chelating effect. All colloids prepared are stable and show no precipitation at room temperature for several months. The catalytic hydrogenations of phenyl aldehydes using the metal colloids as catalysts demonstrate that catalytic activities depend on the variety of the metal colloids and the substrates. The colloidal catalysts stabilized by OAAPS can be recycled by simply adjusting the pH of the solution.

KEY WORDS: platinum; palladium; ruthenium nanoparticles; octa(diacetic aminophenyl) silsesquioxanes; catalytic hydrogenation.

1. Introduction

Owing to the large specific surface area and high catalytic efficiency, using nanoparticles of metals and semiconductors as catalysts have drawn considerable interest in recent years [1–4]. The catalysis of metal nanoparticles has been explored since the pioneering studies of Rampino and Nord in the early 1940s [5]. However, nanoparticles have a tendency to agglomerate, minimizing the interfacial energy of the system. Therefore, various stabilizers used to avoid nanoparticle agglomeration at both the synthetic and catalytic stage have been extensively developed. Many polymers, such as poly (N-vinyl-2-pyrrolidone) [6–10], Carbowax-20 M [11], poly (N-isopropylacrylamide) [12,13], (3-aminopropyl) trimethoxysilane (APS) [14], (poly(acrylic acid) -*b*-polystyrene)₆ [15], sodium polyacrylate [16], dendrimers [17–24], and cubic silsesquioxane [25] have been applied as the stabilizers of nanoparticles. We have reported the preparation and catalysis of metal nanoparticle-cored dendrimers [23,24]. The as-prepared catalyst proved to be effective for the hydrogenation of phenyl aldehydes to phenyl alcohol; however, the activity of the catalyst dropped after a few cycle reactions. This could be attributed to the metal nanoparticles agglomeration, since some of dendrons that attached on the nanoparticle surface were lost in the recycling process. In order to get more stable metal

colloidal catalyst, new stabilizers for preparing the catalysts are still needed.

Polyhedral oligomeric silsesquioxanes have been recognized as well-defined building blocks for nanostructured materials [26–31] and some efficient methods of synthesis have also been developed [32–37]. Cole-Hamilton's group reported a number of rhodium metallodendrimers based on polyhedral oligomeric silsesquioxanes cores that give much higher region-selectivity than their small molecule analogues in the hydroformylation reactions. The positive dendritic effect was explained by the steric crowding and small arm length inducing eight-membered ring bidentate coordination that enhances the selectivity [38–41]. In this paper, we report preparation and catalytic hydrogenation of platinum nanoparticles using octa(diacetic aminophenyl) octasilsesquioxanes (OAAPS) as the stabilizer. Since the OAAPS unit has an inorganic cubic core and eight organic functional groups appended to the vertexes of the cube, we expect it to offer strong bonding to the metal nanoparticles due to chelation.

2. Experimental section

2.1. Materials

3-Methoxybenzaldehyde was purchased from Alfa Aesar. Phenyltrichlorosilane, benzaldehyde, 3-phenoxybenzaldehyde, 4-methoxybenzaldehyde, Methyl chloroacetate, NaBH₄, H₂PtCl₆, HAuCl₄, KI, K₂CO₃, and

*To whom correspondence should be addressed.

E-mail: pyang@suda.edu.cn

organic solvents were obtained from Shanghai Chemical Reagents Company. All the chemical reagents were used without further purification.

2.2. Synthesis of octa(diacetic aminophenyl) silsesquioxane

Octa(aminophenyl) silsesquioxane (OAPS) was synthesized according to methods used in the literature [28,32]. The synthesis of OAAPS is shown in Scheme 1. 0.504 g OAPS (4.34×10^{-4} mol), 1.52 g methyl chloroacetate (1.4×10^{-2} mol), 0.808 g K_2CO_3 (6×10^{-3} mol), and a small piece of KI as catalyst mixed with 10 mL acetone were refluxed for 24 h under magnetic stirring. The resultant mixture was cooled to room temperature and the solvent was removed on a rotary evaporator. The residue was washed with deionized water several times and dried under vacuum to give octa (dimethylacetate aminophenyl) silsesquioxane (OMAAPS). 0.1 g OMAAPS (4.34×10^{-5} mol), 2.78×10^{-2} g NaOH (6.94×10^{-4} mol) mixed with 2 mL ethanol and 10 mL deionized water were refluxed under magnetic stirring for 18 h. Then, the solution was cooled to room temperature and neutralized with diluted hydrochloric acid. The light brown precipitate was washed with deionized water and dried under vacuum. The compound was characterized by ^1H NMR and FTIR. (^1H NMR: (D_2O , 400 MHz) (ppm) δ : 6.525–7.186 (4H, Ar–H), 3.808 (4H, NCH_2COO^-); FTIR: ν (KBr) (cm^{-1}): 2605 (COO^-), 1654 ($\text{C}=\text{O}$), 1078 ($\text{Si}-\text{O}-\text{C}$).

2.3. Preparation of metal nanoparticles stabilized by OAAPS

Platinum nanoparticles stabilized by OAAPS were prepared using NaBH_4 as a reducing agent. 3.9 mmol H_2PtCl_6 and an appropriate amount of OAAPS (the molar ratio of H_2PtCl_6 and OAAPS could be varied from 5 to 25) were dissolved in 10 mL deionized water and the pH of the solution was adjusted to ca. 1.5. Next, 2 mL fresh prepared sodium borohydride solution (0.0579 M) was added dropwise under magnetic stirring. The molar ratio of NaBH_4 and H_2PtCl_6 was 30, to ensure complete reduction of the platinum salt. During

the reduction process, the color of the solution changed from light orange to dark brown. The resulting colloidal solution was dialyzed against deionized water to remove excess NaBH_4 and Cl^- ions. The nanoparticles of palladium, and ruthenium, stabilized by OAAPS were prepared using the same method. For convenience, the samples were labeled as Pt@OAAPS, Pd@OAAPS, and Ru@OAAPS for platinum, palladium, and ruthenium nanoparticles stabilized by OAAPS, respectively.

2.4. Characterization

UV-visible absorption spectra were recorded with a TU1810 SPC spectrophotometer. X-ray diffraction (XRD) patterns were obtained with a Philips diffractometer using Ni-filtered Cu K α radiation. Transmission electron microscopy (TEM) studies were conducted on a TECNAI-G20 electron microscope operating at 200 kV. The sample for TEM analysis was prepared by dropping a drop of the dilute colloidal solution onto a Formvar-covered copper grid and drying in air at room temperature.

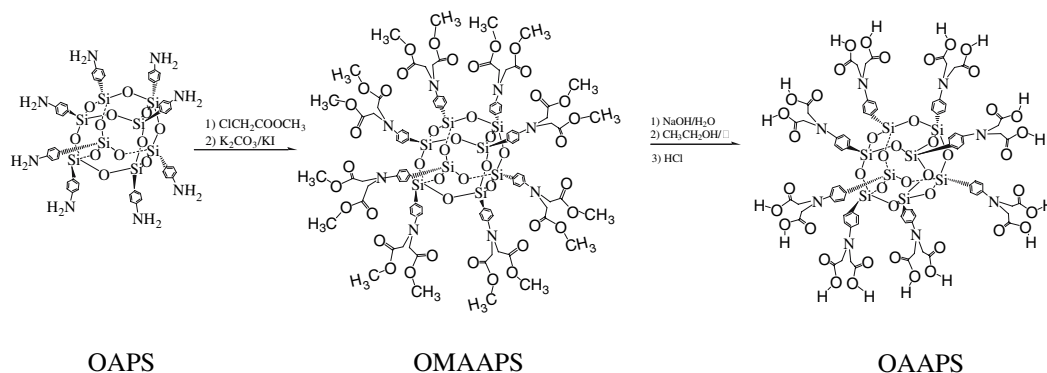
2.5. Catalytic hydrogenation of phenyl aldehydes

Hydrogenation reactions were carried out in a 50 mL three-necked, round-bottomed Schlenk flask equipped with a hydrogen adapter, a dropping funnel, and a reflux condenser with a second adapter connected to a liquid paraffin bubbler. The system was purged with H_2 for 30 min before the reaction. Reactions were carried out by adding 2 mmol of substrate dissolved in the EtOH– H_2O solvent ($\text{EtOH}/\text{H}_2\text{O} = 1$ (v/v)) and 4×10^{-3} mmol of metal colloid as catalyst through the dropping funnel under vigorous stirring conditions. All of the hydrogenation reactions were carried out at 40 °C and atmospheric pressure.

3. Results and discussion

3.1. Pt@OAAPS nanoparticles

Figure 1 shows the UV-visible spectra of the OAAPS- H_2PtCl_6 solution during the reduction process.



Scheme 1. Synthesis of OAAPS.

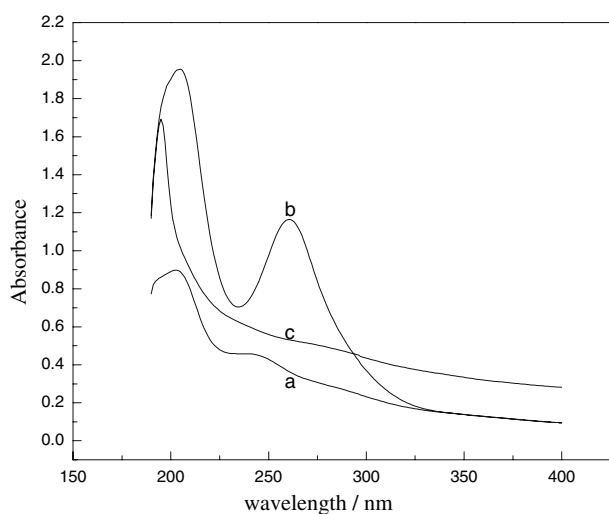


Figure 1. The UV-visible spectra of the OAAPS ethanol aqueous solution (a), the mixture of OAAPS and H_2PtCl_6 before (b), and after reduction (c).

The OAAPS aqueous solution shows an absorption band at 245 nm. The band disappeared after the pH of the solution was adjusted to ca. 1.5. An absorption band centered at 260 nm appeared when the stabilizer and H_2PtCl_6 were mixed together. The band at 260 nm, which can be attributed to platinum ions, disappeared after the reduction of H_2PtCl_6 , indicating that the $[\text{PtCl}_6]^{2-}$ ions are completely reduced. After reduction, the absorption intensity of the spectrum of the solution became much higher throughout the wavelength range measured. This resulted from the interband transition of the encapsulated zerovalent platinum metal particles [18]. The stability of a Pt colloidal solution stabilized by OAAPS strongly depends on the molar ratio of Pt/OAAPS and the pH of the solution. When the molar ratio of platinum and OAAPS was between five and ten, the slightly basic colloidal solution of Pt@OAAPS was

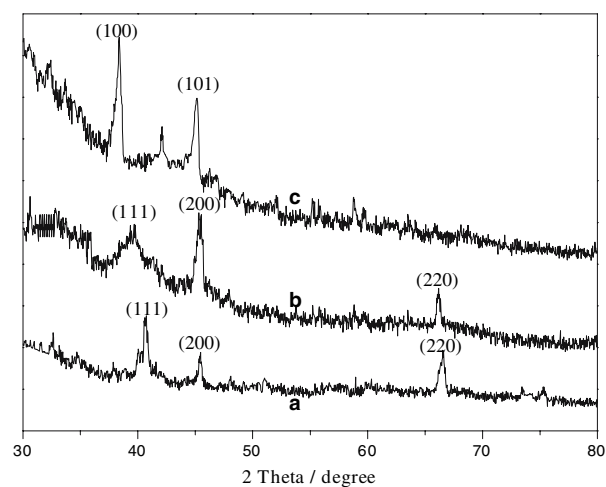


Figure 2. XRD patterns of Pt@OAAPS(a), Pd@OAAPS (b), and Ru@OAAPS (c).

stable without precipitation at room temperature for more than 1 year.

The formation of OAAPS-stabilized platinum nanoparticles can also be confirmed by the XRD patterns of samples (figure 2 curve a). The XRD patterns of the sample showed the characteristic diffraction peaks of the platinum face-centered cubic phase, indicating the formation of metallic platinum [42,43].

Figure 3 shows a TEM image of Pt@OAAPS (the molar ratio of H_2PtCl_6 and OAAPS is 7) and the corresponding core-size distribution histogram. It can be seen from the figure that the platinum particles are small and the core sizes exhibit a relatively narrow size distribution (1–2.4 nm). The average diameter and dispersivity obtained from the histogram plot are 1.6 ± 0.3 nm.

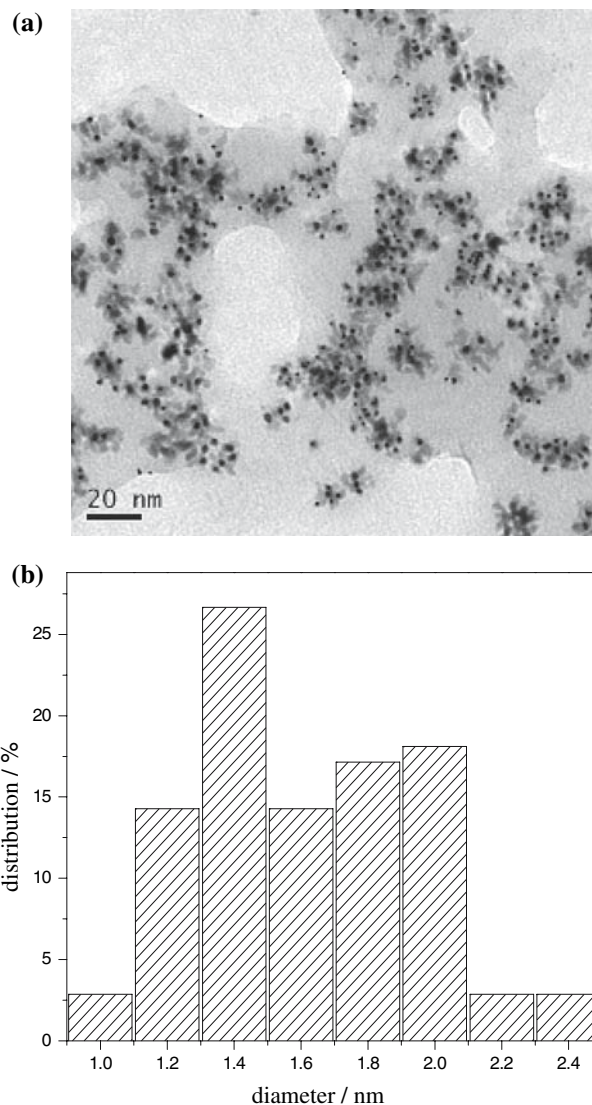


Figure 3. TEM image of Pt@OAAPS nanoparticles (a), and the corresponding core-size distribution histogram (b). The average size and standard deviation of the particles are 1.6 ± 0.3 nm. The molar ratio of Pt/OAAPS is 7.

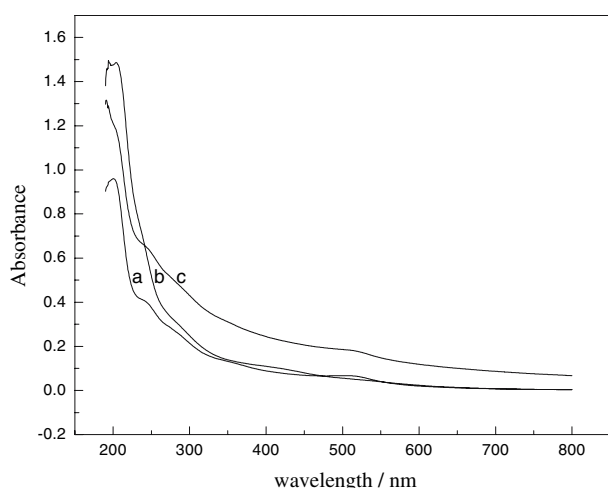


Figure 4. The UV-visible spectra of the OAAPS ethanol aqueous solution (a), the mixture of OAAPS and H_2PdCl_4 before (b), and after reduction of H_2PdCl_4 (c).

3.2. Pd@OAAPS nanoparticles

The UV-visible spectra of OAAPS- H_2PdCl_4 in aqueous solution before and after reduction with sodium borohydride are shown in figure 4. Although there is no characteristic surface plasmon band of Pd (0) nanoparticles, the spectrum shows an increasing absorption at increasing energy due to the scattering of Pd nanoparticles [44]. The color of the solution turned from orange to dark brown after the reduction. Like the Pt@OAAPS, the stability of OAAPS capped Pd (0) nanoparticles depends on the molar ratio of Pd/OAAPS. The dark brown solution of Pd@OAAPS in which the range of the molar ratio of H_2PdCl_4 /OAAPS was from 10 to 30 was stable without precipitation at room temperature for several months.

The X-ray powder diffraction pattern of the resulting sample confirmed the face centered cubic structure of the metallic Pd (figure 2 curve b). The TEM image (figure 5) shows a narrow size distribution of palladium nanoparticles (the molar ratio of H_2PdCl_4 and OAAPS is 7). The average diameter and dispersivity obtained from the histogram plot are 1.4 ± 0.2 nm.

3.3. Ru@OAAPS Nanoparticles

The UV-visible spectrum of the freshly prepared aqueous solution of RuCl_3 consists of the peaks at 312 and 500 nm (figure 6). These two peaks can be attributed to the ruthenium-water and/or chlorine ions complex [45]. When the solution of OAAPS was mixed with RuCl_3 solution, no new peaks were detected. This may be interpreted as being the result of no strong Ru^{3+} ions complexing with OAAPS. After reduction of Ru (III) by sodium borohydride, the color of the solution turned from brown to dark black. The UV-vis spectrum of the solution shows an increasing absorption at increasing energy. The dark black colloidal solution of Ru@OA-

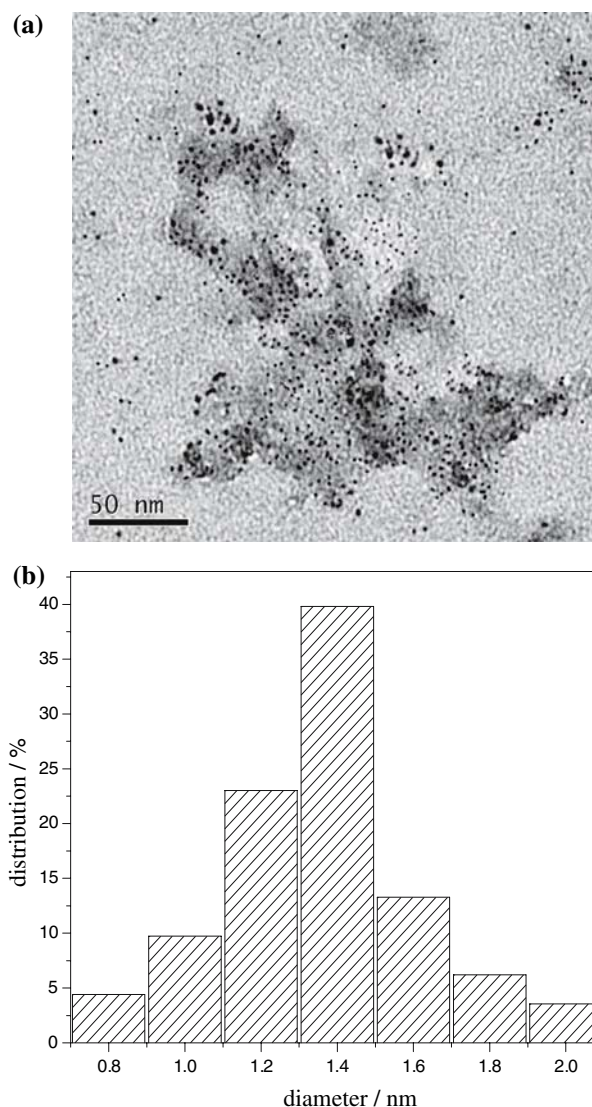


Figure 5. TEM image of Pd@OAAPS nanoparticles (a), and the corresponding core-size distribution histogram (b). The average size and standard deviation of the particles are 1.4 ± 0.2 nm. The molar ratio of Pd/OAAPS is 7.

APS in which the range of the molar ratio of RuCl_3 /OAAPS was from 10 to 25 was stable without precipitation at room temperature for several weeks. XRD confirmed that the formation of metallic ruthenium had occurred (figure 2 curve c) [46].

Figure 7 presents the TEM image of Ru nanoparticles stabilized by OAAPS (the molar ratio of RuCl_3 and OAAPS is 7) and the corresponding core-size distribution histogram. The average diameter and dispersivity obtained from the histogram plot are 1.3 ± 0.2 nm. The stability and the size of OAAPS capped Ru (0) nanoparticles depend on the molar ratio of Ru/OAAPS. For Ru@OAAPS, the average diameter of Ru (0) particles changed from 1.3 to 1.9 nm when the molar ratio of RuCl_3 /OAAPS changed from 7 to 10.

FTIR spectra of samples (figure 8) show there are about $15\text{--}25\text{ cm}^{-1}$ peak shift to low wavenumber

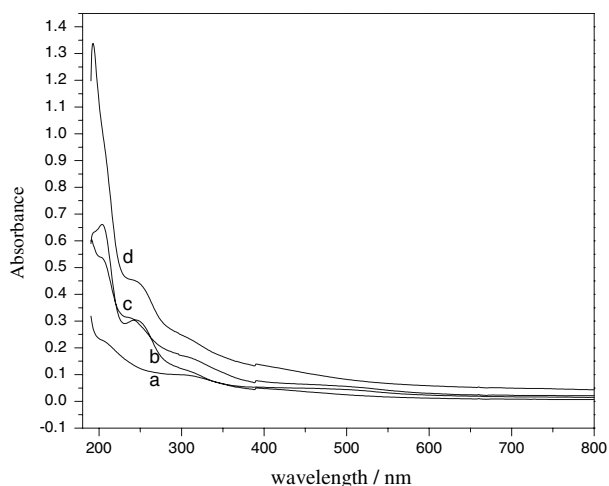


Figure 6. The UV-visible spectra of RuCl_3 aqueous solution (a), the OAAPS solution (b), the mixture of RuCl_3 and OAAPS before (c), and after reduction (d).

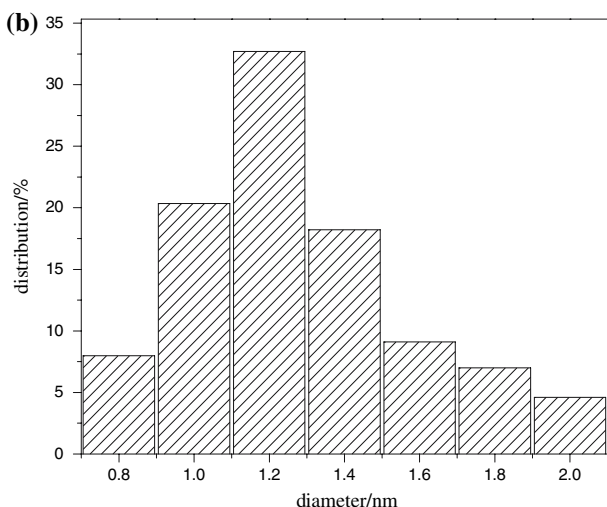
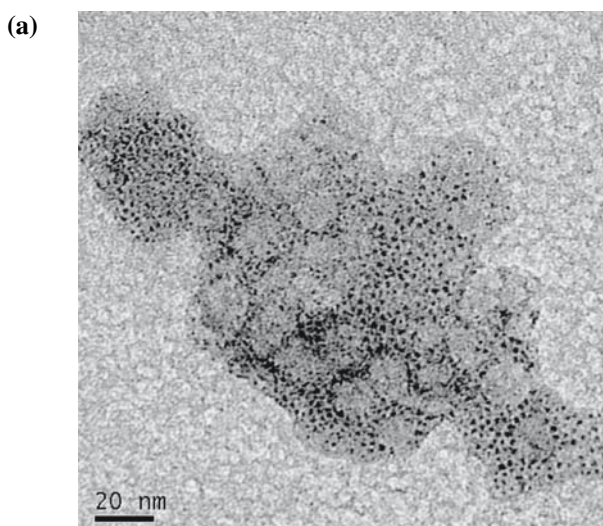


Figure 7. TEM image of Ru@OAAPS nanoparticles (a), and the corresponding core-size distribution histogram (b). The average size and standard deviation of the particles are 1.3 ± 0.2 nm (b). The molar ratio of Ru/OAAPS is 7.

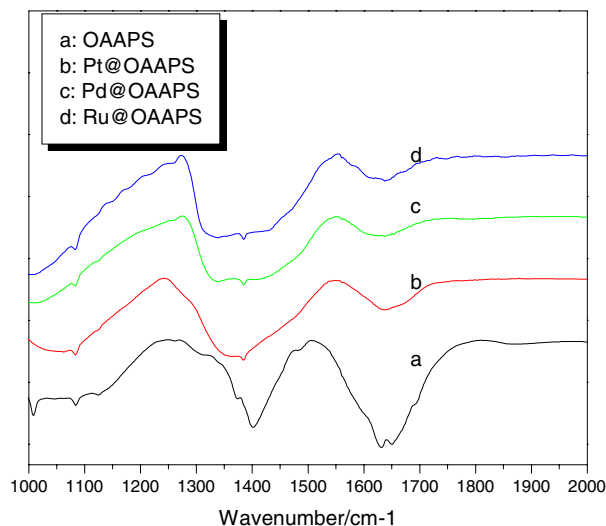
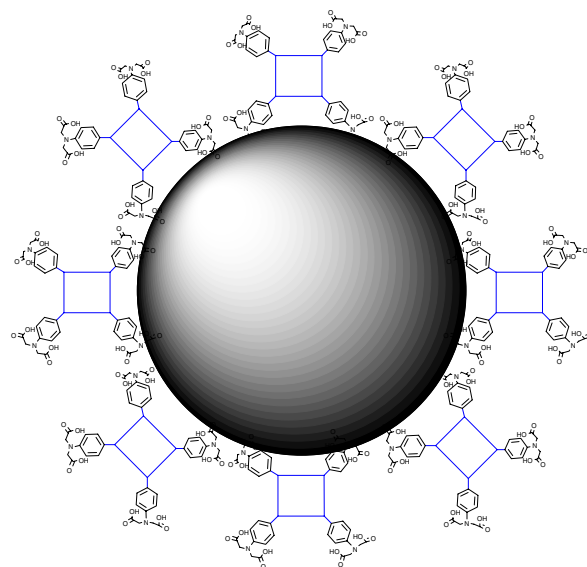


Figure 8. FTIR spectra of OAAPS (a), Pt@OAAPS (b), Pd@OAAPS (c), and Ru@OAAPS (d).

comparing the $\text{C}=\text{O}$ band stretching vibration of M@OAAPS with that of OAAPS in salt form. The significant peak shift for M@OAAPS is the evidence of the interaction between metal cluster and carboxyl-terminated OAAPS [47] since the $\text{C}=\text{O}$ bond have less electron density as the oxygen atom of the carbonyl interacted with the surface atom of the metal nanoparticles. The supposed configuration of M@OAAPS is shown in Scheme 2.

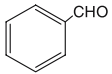
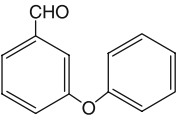
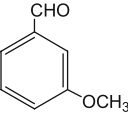
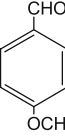
3.4. Catalytic reduction of phenyl aldehydes

The hydrogenation of phenyl aldehydes was chosen to be the model reaction to investigate the catalytic



Scheme 2. Supposed configuration of metal colloid stabilized by OAAPS. The black square is a 2D representation of the cubic core of the silsesquioxane.

Table 1
Catalytic activity of metal OAAPS for hydrogenation of phenyl aldehydes

Substrate	Catalyst	Time (h)	Conversion (%)	TOF (mole product per mole metal per hour)
	Pt@OAAPS	16	88.2	28
	Pd@OAAPS	3.5	98.5	143
	Ru@OAAPS	16	10.9	3
	Pt@OAAPS	16	98.7	31
	Pd@OAAPS	16	24.6	8
	Ru@OAAPS	16	22.0	6
	Pt@OAAPS	16	22.5	7
	Pd@OAAPS	16	13.6	4
	Ru@OAAPS	16	15.4	5
	Pt@OAAPS	16	0.6	0.2
	Pd@OAAPS	16	90.1	28
	Ru@OAAPS	16	~0	~0

Reaction conditions: solvent: ethanol/water = 1 (v/v); catalyst: metal@OAAPS ($n_{\text{metal}}/n_{\text{OAAPS}} = 10$); $n_{\text{substrate}}/n_{\text{catalyst}} = 500$; reaction temperature: 40 °C.

activities of as-prepared metallic colloids. The reduction process of the substrates can be visualized through the descending of the absorption peaks between 277 and 310 nm. Details about the catalytic hydrogenation are summarized in Table 1. The catalytic activity depends on the catalysts and the substrates. Pt@OAAPS can be used as the catalyst for the hydrogenation of benzaldehyde and 3-phenoxybenzaldehyde. The Pd@OAAPS colloid was found to be effective for the hydrogenation of

benzaldehyde and 4-methoxybenzaldehyde while Ru@OAAPS seemed to not be a suitable catalyst for hydrogenation of phenyl aldehydes. The temporal processes of the catalytic hydrogenations are shown in figure 9. Comparing the catalytic activities of metal colloids stabilized by OAAPS with those of platinum nanoparticles stabilized by polyaryl ether aminediacetic acid dendrimer (Pt-G_nNAs) [24], it was found that Pt-G_nNAs are more active for the hydrogenation of phenyl aldehydes than the metal colloids stabilized by OAAPS. This could be attributed to the fact that a

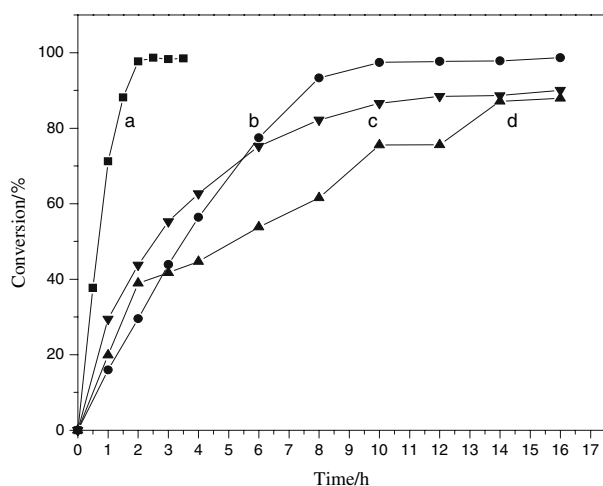


Figure 9. The conversion rate of the hydrogenation of phenyl aldehydes (a), benzaldehyde catalyzed by Pd@OAAPS (b), 3-phenoxybenzaldehyde catalyzed by Pt@OAAPS (c), 4-methoxybenzaldehyde catalyzed by Pd@OAAPS (d), benzaldehyde catalyzed by Pt@OAAPS. Reaction conditions: [metal]/[OAAPS] = 10; [substrate]:[metal] = 500; Reaction temperature: 40 °C.

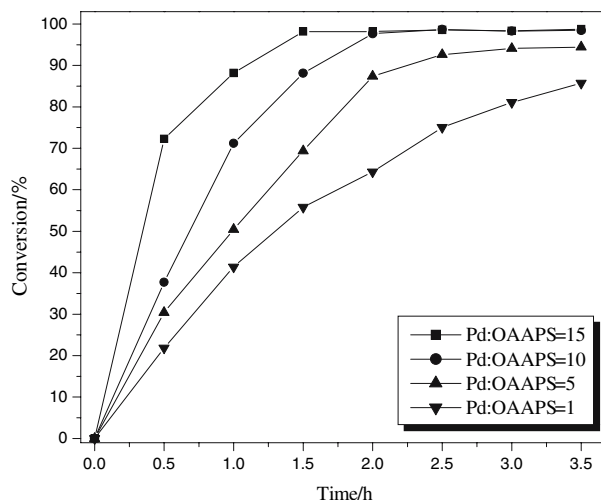


Figure 10. The influence of the molar ratio of Pd/stabilizer on the hydrogenation of benzaldehyde. Reaction conditions: Catal: Pd@OAAPS; [substrate]:[metal] = 500; Reaction temperature: 40 °C.

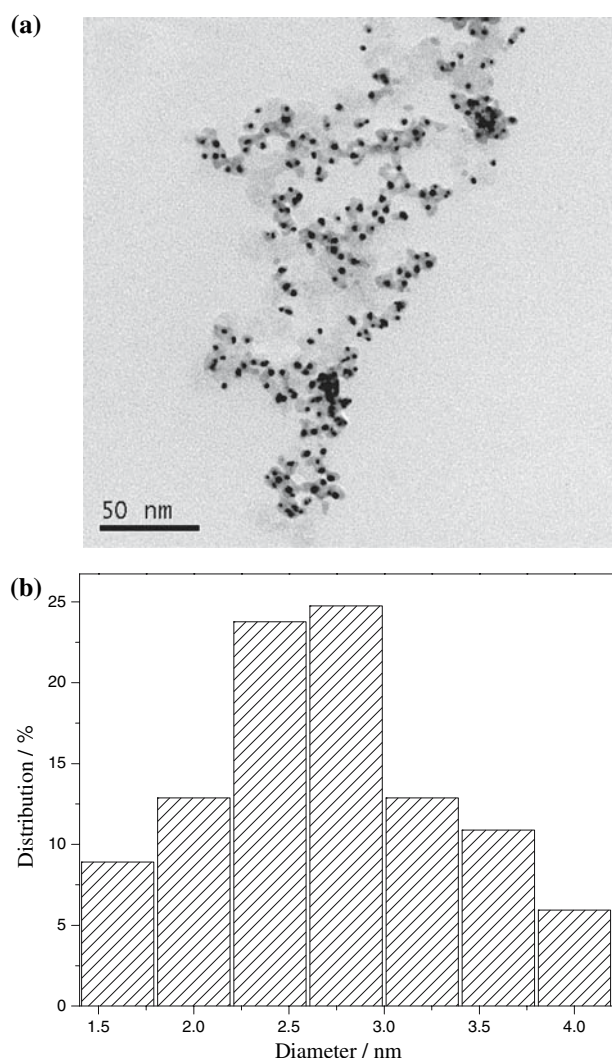


Figure 11. TEM image and corresponding histogram of size distribution of Pd@OAAPS nanoparticles used and recycled for eight times.

substantial fraction of the surface of the metal nanoparticle stabilized by polyaryl ether dendrons is unpassivated and available for catalysis, while a relatively less unpassivated particle surface is left for nanoparticles stabilized by OAAPS, since one OAAPS molecule can coordinate with the metal nanoparticle through half of its eight organic functional arms appended to the vertexes of the cubic silica core. The surface area of the metal nanoparticle covered by OAAPS molecules seems to be unavailable for catalytic hydrogenation. We posit that a silsesquioxane core with longer organic arms would give the metal colloids greater catalytic activity, since the coving effect will be reduced.

The hydrogenation of benzaldehyde was employed to investigate the influence of the ratio of palladium metal to the stabilizer on the catalytic activity of Pd@OAAPS. The results are demonstrated in figure 10. It can be concluded from figure 10 that the catalytic activity increases with the increasing of the molar ratio of the metal to the stabilizer. The larger the ratio of the metal

to the stabilizer is, the greater the surface of the metal nanoparticle left for catalysis is.

The accessible surface area of the nanoparticles stabilized by OAAPS may be further investigated by using substrates in different molecular size. It is expected that the nanoparticles with a large accessible surface area should be available as a catalyst to the substrates in different molecular size while the nanoparticles with a small accessible surface area will only be suitable to the substrates in small size. The work on the accessible surface area of nanoparticles is still under way.

It is interesting to note that OAAPS stabilized metal colloids could be precipitated by lowering the pH of the solution; the precipitate could be redissolved in a slightly basic alcohol aqueous solvent. This provides a convenient method for the recycling of the catalyst. Pd@OAAPS catalyst can be recovered and recycled eight times without obvious loss of the catalytic activity. Figure 11 shows TEM image and corresponding histogram of size distribution of Pd@OAAPS nanoparticles used and recycled for eight times. The average diameter and dispersity obtained from the histogram plot are 2.7 ± 0.5 nm. The mean diameter of nanoparticles increased slightly after catalytic reaction. The fact indicates that OAAPS is a nice stabilizer to prevent metal nanoparticles agglomeration in the catalytic reaction process.

4. Conclusions

Platinum, palladium, and ruthenium colloids were successfully prepared using octa(dimethylacetate aminophenyl) silsesquioxane as the stabilizer. The as-prepared colloids show excellent stability since OAAPS offers stronger bonding of the cubic linker to the metal nanoparticles due to chelation. Pt and Pd nanoparticles stabilized by OAAPS can be used as catalysts for the hydrogenation of some phenyl aldehydes, though the catalytic activities of the colloids are not as high as those of the metal nanoparticles stabilized by polyaryl ether dendrons. The colloidal catalysts stabilized by OAAPS can be recycled by simply adjusting the pH of the solution.

Acknowledgments

This research was supported by the National Natural Science Foundation of China (20673075, 20553001, and 50673070). The authors are grateful to Professor R. M. Laine (Michigan University) for his valuable suggestions for the synthesis of OAPS.

References

- [1] A. Henglein, Chem. Rev. 89 (1989) 1861.
- [2] G. Schmid, Chem. Rev. 92 (1992) 1709.
- [3] L.N. Lewis, Chem. Rev. 93 (1993) 2693.

- [4] D. Astruc, F. Lu and J.R. Aranzaes, *Angew. Chem. Int. Ed.* 44 (2005) 7852.
- [5] L.D. Rampino and F.F. Nord, *J. Am. Chem. Soc.* 63 (1941) 2745.
- [6] P. Lu, J. Dong and N. Toshima, *Langmuir* 15 (1999) 7980.
- [7] D.G. Duff, P.P. Edwards and B.F.G. Johnson, *J. Phys. Chem.* 99 (1995) 15934.
- [8] R. Narayanan and M.A. El-Sayed, *J. Am. Chem. Soc.* 125 (2003) 8340.
- [9] M. Liu, B. He, H. Liu and X. Yan, *J. Colloid Interf. Sci.* 263 (2003) 461.
- [10] S.H. Choi, Y.P. Zhang, A. Gopalan, K.P. Lee and H.D. Kang, *Colloid Surf. A* 256 (2005) 165.
- [11] P.A. Brugger, P. Cuendet and M. Grätzel, *J. Am. Chem. Soc.* 103 (1981) 2923.
- [12] C.W. Chen and M. Akashi, *Langmuir* 13 (1997) 6465.
- [13] M. Akane and N. Yoshio, *Langmuir* 16 (2000) 7109.
- [14] D. Nagao, Y. Shimazaki, Y. Kobayashi and M. Konno, *Colloid Surf. A* 273 (2006) 97.
- [15] L. Zhang, H. Niu, Y. Chen, H. Liu and M. Gao, *J. Colloid Interf. Sci.* 298 (2006) 177.
- [16] T. Toshiharu, K. Ryo and M. Mikio, *J. Inorg. Organo. Poly.* 10 (2000) 145.
- [17] K. Esumi, R. Isono and T. Yoshimura, *Langmuir* 20 (2004) 237.
- [18] R.M. Crooks, M. Zhao, L. Sun, V. Chechik and L. Yeung, *Acc. Chem. Res.* 34 (2001) 181.
- [19] E.H. Rahim, F.S. Kamounah, J. Frederiksen and J.B. Christensen, *Nano Lett.* 1 (2001) 499.
- [20] Y. Li and M.A. El-Sayed, *J. Phys. Chem. B* 105 (2001) 8938.
- [21] M. Ooe, M. Murata, T. Mizugaki, K. Ebitani and K. Kaneda, *Nano Lett.* 2 (2002) 999.
- [22] K.R. Gopidas, J.K. Whitesell and M.A. Fox, *J. Am. Chem. Soc.* 125 (2003) 6491.
- [23] Y. Du, W. Zhang, X. Wang and P. Yang, *Catal. Lett.* 107 (2006) 177.
- [24] P. Yang, W. Zhang, Y. Du and X. Wang, *J. Mol. Catal. A: Chem.* 260 (2006) 4.
- [25] K. Naka, H. Itoh and Y. Chujo, *Nano Lett.* 2 (2002) 1183.
- [26] L. Zheng, S. Hong, G. Cardoen, E. Burgaz, S.P. Gido and E.B. Coughlin, *Macromolecules* 37 (2004) 8606.
- [27] J. Choi, J. Harcup, A.F. Yee, Q. Zhu and R.M. Laine, *J. Am. Chem. Soc.* 123 (2001) 11420.
- [28] R. Tamaki, Y. Tanaka, M.Z. Asuncion, J. Choi and R.M. Laine, *J. Am. Chem. Soc.* 123 (2001) 12416.
- [29] T. Cassagneau and F. Caruso, *J. Am. Chem. Soc.* 124 (2002) 8172.
- [30] R. Tamaki, J. Choi and R.M. Laine, *Chem. Mater.* 15 (2003) 793.
- [31] H. Mori, M.G. Lenzendörfer, A.H.E. Müller and J.E. Klee, *Macromolecules* 37 (2004) 5228.
- [32] R.M. Laine, R. Tamaki and J. Choi WO 02/100867 A1.
- [33] R.H. Baney, M. Itoh, A. Sakakibara and T. Suzuki, *Chem. Rev.* 95 (1995) 1409.
- [34] G.Z. Li, H. Cho, L. Wang, H. Toghiani and C.U. Pittman, *J. Poly. Sci. A* 43 (2005) 355.
- [35] J. Choi, S.G. Kim and R.M. Laine, *Macromolecules* 37 (2004) 99.
- [36] N. Maxim, P. Magusin, P.J. Kooyman, J. Wolput, R. Santen and H. Abbenhuis, *Chem. Mater.* 13 (2001) 2958.
- [37] P.-A. Jaffrès and R.E. Morris, *J. Chem. Soc., Dalton Trans.*, (1998) 2767.
- [38] L. Ropartz, R.E. Morris, D.F. Foster and D.J. Cole-Hamilton, *Chem. Commun.* (2001) 361.
- [39] L. Ropartz, D.F. Foster, R.E. Morris, A.M.Z. Slawin and D.J. Cole-Hamilton, *J. Chem. Soc., Dalton Trans.* 1997 (2002).
- [40] L. Ropartz, R.E. Morris, D.F. Foster and D.J. Cole-Hamilton, *J. Mol. Catal. A: Chem.* 182–183 (2002) 99.
- [41] L. Ropartz, K.J. Haxton, D.F. Foster, R.E. Morris, A.M.Z. Slawin and D.J. Cole-Hamilton, *J. Chem. Soc., Dalton Trans.*, (2002) 4323.
- [42] T. Teranishi, M. Hosoe, T. Tanaka and M. Miyake, *J. Phys. Chem. B* 103 (1999) 3818.
- [43] S. Chen and K. Kimura, *J. Phys. Chem. B* 105 (2001) 5397.
- [44] C. Wang, D. Chen and T. Huang, *Colloid Surf. A* 189 (2001) 145.
- [45] G. Lafaye, C.T. Williams and M.D. Amiridis, *Catal. Lett.* 96 (2004) 43.
- [46] A. Salomonsson, R.M. Petoral, K. Uvdal, C. Aulin, P. Käll, L. Ojamäe, M. Strand, M. Sanati and A.L. Spetz, *J. Nano. Res.* 8 (2006) 899.
- [47] J. Petroski and M.A. El-Sayed, *J. Phys. Chem. A* 107 (2003) 8371.